Photophysics of First Generation Photomolecular Motors: Resolving Roles of Temperature, Friction and Medium Polarity

Palas Roy[1], Andy Sardjan[2], Wojciech Danowski[3], Wesley R. Browne[2], Ben. L. Feringa[*3] and Stephen R. Meech[*1]

[1] *School of Chemistry, University of East Anglia, Norwich Research Park, Norwich NR4 7TJ, UK*

[2] *Molecular Inorganic Chemistry, Stratingh Institute for Chemistry, University of Groningen, Nijenborgh 4, 9747AG Groningen, The Netherlands*

[3]*Centre for Systems Chemistry, Stratingh Institute for Chemistry, University of Groningen, Nijenborgh 4, 9747AG Groningen, The Netherlands*

Abstract

Light driven unidirectional molecular rotary motors have the potential to power molecular machines. Consequently, optimizing their speed and efficiency is an important objective. Here we investigate factors controlling the photochemical yield of the prototypical unidirectional rotary motor, a sterically overcrowded alkene, through a detailed investigation of its excited state dynamics. An isoviscosity analysis of the ultrafast fluorescence decay data resolves friction from barrier effects and reveals a 3.4±0.5 kJ mol^{-1} barrier to excited state decay in nonpolar media. Extension of this analysis to polar solvents shows that this barrier height is a strong function of medium polarity, and that the decay pathway becomes near barrierless in more polar media. Thus, the properties of the medium can be used as a route to controlling the motor's excited state dynamics. The connection between these dynamics and the quantum yield of photochemical isomerization is probed. The photochemical quantum yield is shown to be a much weaker function of solvent polarity, and the most efficient excited state decay pathway does not lead to a strongly enhanced quantum yield for isomerization. These results are discussed in terms of the solvent dependence of the complex multidimensional excited state reaction coordinate.

* Authors for correspondence: s.meech@uea.ac.uk; b.l.feringa@rug.nl

Keywords. Excited state, molecular motor, photoisomerisation, ultrafast fluorescence dynamics, isoviscosity, activation energy, quantum yield.

Introduction

Machines are assemblies of components capable of directed and controllable mechanical motion. The complex molecular machines found in biology inspired chemists to develop synthetic molecular machines, with the aim of reliably and reproducibly controlling molecular motion at the nanoscale.[1-2] A key component for the development of molecular machines will be the motor, a power source that must be capable of overcoming Brownian motion to yield the directional molecular motion required. The number of functional molecular machines is growing, and they have been variously powered by electron injection, light and chemical reaction. [2-8]

In this work the focus is on molecular motors powered by the absorption of light, more specifically photo-activated unidirectional rotation about double bonds.[3-4, 9] Numerous molecular switches, and some of the earliest molecular machines, employed cis-trans isomerization in – for example –stilbene and azobenzene based chromophores.[10-11] While such classical photochemical isomerization reactions yield control over molecular shape and, when coupled to other molecules, intermolecular distance, they do not permit control over the direction of rotation. The problem of obtaining directional rotational motion was solved by Feringa and co-workers, through exploitation of double bond isomerization in sterically overcrowded alkenes.[12-13] In the first generation of such motors the photoactive double bond links two identical units, each of which has a chiral centre; the photocycle is shown in Figure 1.[13] Electronic excitation of the cis form initiates an isomerization reaction to populate a trans form, which inverts the helicity of the molecule. This yields a ground state structure with a thermodynamically unfavorable pseudo equatorial orientation of the methyl groups. This metastable state undergoes a thermal helix inversion, to yield the stable trans configuration with axially oriented methyl groups. Absorption of a second photon stimulates the trans to cis excited state isomerization, to yield a metastable cis form which undergoes a second thermal helix inversion to yield the complete 360° rotation (Figure 1).

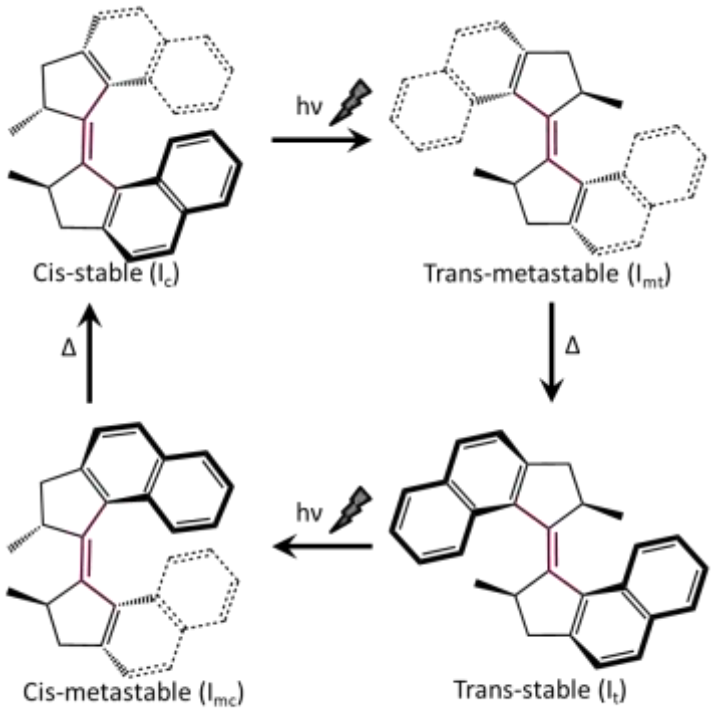

Figure 1. Photocycle of first-generation molecular motor.

Steady state photochemical measurements revealed that the photochemical isomerization reactions are reversible, and that the photostationary state favors the metastable product. The rate limiting process for the rate of rotation is the ground state thermal helix inversion, which has a high activation barrier, leading to low overall rotation rates.[14] A critical redesign resulted in a second generation of photomolecular motors, in which the tricyclic moieties connected by the double bond are structurally distinct – called the rotor and the stator.[15] The rotor contains a chiral centre and is of similar structure to one half of the first generation motor, with the stator typically being a xanthene or fluorene. These second generation motors not only exhibit lower barriers to thermal helix inversion, leading to faster rotation rates of up to 1 MHz, but are also more amenable to synthetic variation (for example attachment of the stator to a surface[16-17]) and require only a single chiral centre.[18-19] In general a disadvantage of the second generation motors is that the position of the photostationary state is typically less favorable than for the first generation, and the yield of the photochemical isomerization is

significantly lower.[20-22] It is expected, and has been shown theoretically,[23-24] that the overall rotation speed will be a product of the photochemical quantum yield and rate of thermal helix inversion (provided these two are well separated in their timescales). Consequently, an ideal motor would combine the high photochemical quantum yield of the first generation with the fast thermal helix inversion of the second generation. Previously we undertook a detailed analysis of excited state processes in second generation motors, through ultrafast electronic and vibrational spectroscopy.[20, 25-27] The excited state isomerization mechanism was characterized, and it was shown that some simple chemical substitutions modified the photochemical yield and excited state dynamics.[20] More recently, the excited state dynamics of the first generation motors have been under similarly detailed investigation, and are the focus of this work.[28-29] The objectives of the present study are to understand factors controlling excited state dynamics in first generation motors, and especially to investigate means of modifying them through medium effects.

To this end, the solvent dependence of the excited state dynamics of the first generation motor, dimethyl tetrahydro- bi(cyclopenta[α]napthal-enylidene), **I** (shown in Figure 1) are measured. The photodynamics of **I** were previously investigated by ultrafast transient absorption and fluorescence up-conversion.[28-29] Using transient absorption Sension et al studied all four states of the motor (Figure 1) and, for $\mathbf{I_c}$, uncovered a sub-picosecond relaxation on the excited state surface which populated a more weakly emissive state, which subsequently undergoes a multistep decay to the ground state.[28] In a time resolved fluorescence study of the stable cis ($\mathbf{I_c}$) to metastable trans ($\mathbf{I_{mt}}$) photochemical reaction (Figure 1) we resolved a 100 fs decay of a blue shifted Franck-Condon excited state, which relaxes into the fluorescent state, accompanied by excitation of coherently excited vibrational modes, which are damped on the sub-picosecond time scale. The relaxed excited state itself undergoes a multi-exponential decay, with a rate that is a function of medium friction. The significant differences observed between these excited state dynamics and those reported earlier for the second generation motors,

were suggested to reflect the existence of a barrier on the excited state surface in **I**.[29] Together, these results point to a significant role for the solvent in determining the excited state dynamics, but the origin of that solvent dependence has not yet been addressed in detail. The solvent effect requires proper characterization, because controlling the polarity and viscosity of the medium independently offer a potential route to optimizing the efficiency of motor operation.

To achieve the desired characterization, we describe a study of the excited state decay of the cis-stable form, $\mathbf{I}_c$, in both nonpolar (alkane) and polar (alcohol) solvents. We present a detailed isoviscosity analysis of the ultrafast fluorescence,[30-32] which allows the separation of friction from thermal activation effects, both of which contribute to determining the rate of the excited state reaction. Our data reveal the predicted barrier to decay of the emissive state in nonpolar solvents. Extension of the same analysis to polar solvents reveals an important and unexpected role for solvent polarity in determining the excited state dynamics. These results are discussed in terms of the nature of the reaction coordinate, and in particular the role of sudden polarization, as previously identified in some classical photochemical isomerization reactions.[33-35] We use these new results as the basis for a reinvestigation of the quantum yield of isomerization in $\mathbf{I}_c$, and show that the solvent dependence of the excited state dynamics does not play a dominant role in determining motor efficiency.

Experimental Methods

$\mathbf{I}_c$ was synthesized and purified as previously described.[13] Spectroscopic characterization of $\mathbf{I}_c$ is described in supporting information. Fluorescence lifetimes were measured using a fluorescence up-conversion technique with 50 fs time resolution;[36] further details are given in supporting information. Absolute photoconversion quantum yields were determined, as detailed in supporting information.

Results

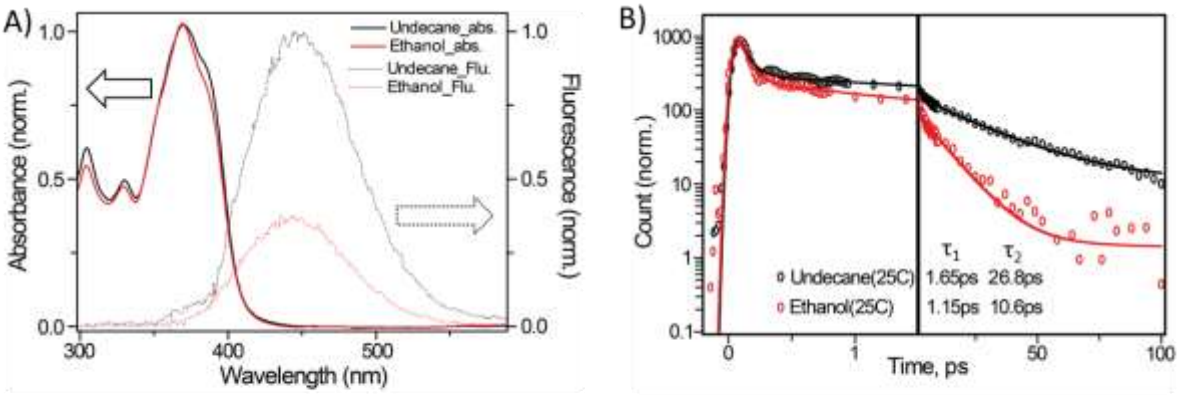

Figure 2. a) Steady-state absorption, emission (excitation at 355 nm) of $\mathbf{I_c}$. Emission data are corrected for absorbance b) Time-resolved emission kinetics of $\mathbf{I_c}$ in Undecane (black) vs ethanol (red) at 465 nm at room temperature . The solid line is a fit to two exponential decay terms (τ_1, τ_2) plus a small constant offset .

Steady State and Time Resolved Electronic Spectra. Figure 2A compares the steady state absorption and fluorescence spectra for $\mathbf{I_c}$ in polar ethanol (ε_r = 25.3) and nonpolar undecane (ε_r = 2.0) solutions; these solvents were selected to have near identical viscosities (1.1 mPa s) at 298 K. The absorption spectra differ only in a slightly better resolved shoulder for undecane. This small difference may arise from differences in line broadening mechanisms in the two solvents, although it could also indicate a modified Franck Condon state. The fluorescence data reveal a solvent polarity dependent radiationless decay, with the emission being more strongly quenched in the polar ethanol solvent. This polarity effect is evidently in addition to the previously characterized medium viscosity dependence.[29] The polarity dependent fluorescence quenching is not accompanied by any significant solvent dependence of either the maximum wavelength or the spectral shape of the electronic spectra. This is illustrated in more detail in supplementary information for a wider range of solvents (Figure S7). Thus, there is no evidence from these steady state data for formation of an intramolecular charge transfer (CT) state on population of the emissive state of $\mathbf{I_c}$, since such a change in permanent dipole moment would lead to significant solvatochromism.

The time resolved fluorescence data for the same pair of solvents are shown in Figure 2B. The profile of the time resolved fluorescence of $\mathbf{I_c}$ was previously described.[29] In agreement with the earlier data,

there is a ca 100 fs decay of the sterically strained Franck-Condon (FC) state in both solvents, suggesting that any change in the FC state (Figure 2A) does not modify the dynamics. This ultrafast FC state relaxation leads to a fluorescent state, which has a picosecond timescale decay and a reduced transition dipole moment. The decay is accompanied by an oscillation in the fluorescence profile, ascribed to coherent excitation of low frequency Raman active vibrational modes in the excited electronic state, which are damped on the sub-picosecond timescale. A Fourier transform analysis of this oscillatory feature shows that the frequency associated with these low-frequency modes are solvent-polarity independent (see Supporting information S5) indicating that they are not directly involved in the reaction coordinate, but are 'spectator' modes.

The relaxed fluorescent state of $\mathbf{I_c}$ decays with non-single exponential wavelength dependent kinetics.[29] The decay is well fit by a biexponential decay function (Figure 2B, Tables S1,2) plus a small (ca 1%) longer lived component which is not accurately resolved in the current time range, and is fit with an arbitrary long component (> 1 ns). The data in Figure 2B show that the polarity dependent quantum yield (Figure 2A) reflects a change in the radiationless decay rate, with both fast and slow relaxation times becoming faster in the more polar solvent. This quenching is most significant for the slower component, where the decay is accelerated by a factor of about three, a value which is consistent with the steady state fluorescence quenching (Figure 2A).

Isoviscosity Analysis. The picosecond timescale fluorescence decay is assumed to arise from an excited state reaction of the relaxed excited state of $\mathbf{I_c}$ (formed in 100 fs, Fig. 2) resulting in internal conversion to the electronic ground state, where either the product $\mathbf{I_{mt}}$ is formed, or the initial ground state is recovered. Since the excited state lifetime is a few picoseconds, compared with the nanosecond radiative decay rate constant predicted from the extinction coefficient,[37] the mean lifetime of the fluorescence, τ_f, can be taken as a measure of the quenching, and hence of the excited state reaction,

rate constant, $\tau_f^{-1} \sim k_{reac}$. To resolve the viscosity, polarity and temperature dependence of k_{reac} we performed an isoviscosity analysis in both nonpolar alkane and polar n-alcohol solvents; full data is presented in supporting information, Tables S1-S2. [32]

Kramers treatment of a particle diffusing over a barrier has been widely adopted as a representation of a chemical reaction in solution occurring over an activation barrier along a single generalized reaction coordinate. If the friction experienced by the particle is represented by the solvent viscosity (hydrodynamic approximation) then Kramers' theory yields,[32, 38-39]

$$k_{reac} = F(\eta) exp\left(-\frac{E_b}{RT}\right) \qquad (1)$$

Where E_b is the barrier height along the reaction coordinate and $F(\eta)$ is

$$F(\eta) = \frac{\omega_r \eta}{4\pi\omega_b I_r}\left\{\left[1 + \left(\frac{\omega_b I_r}{\eta}\right)^2\right]^{1/2} - 1\right\} \qquad (2)$$

in which ω_r and ω_b are the frequencies characterizing the shape of the harmonic reactant well and the barrier respectively, and I_r is the reduced moment of inertia for the particle on the reaction coordinate. Equation (1) shows directly the problem of extracting E_b from an Arrhenius analysis of the temperature dependent decay time. The viscosity is itself temperature dependent, and (sufficiently far above the glass transition temperature) is often exponentially activated, $\eta = \eta_\infty e^{E_{visc}/RT}$, such that an Arrhenius analysis of τ_f^{-1} yields some mixture of the true activation barrier along the reaction coordinate, E_b, with the activation energy for viscous flow, E_{visc}. This problem may be resolved through an isoviscosity analysis, in which the reaction rate is measured in a series of similar solvents (similar so as to minimize any role for specific solvent effects) with the temperature of each solution being adjusted to yield the same viscosity.[31] In that case an Arrhenius analysis of the temperature dependence yields E_b, directly, and thus $F(\eta)$ can be resolved.

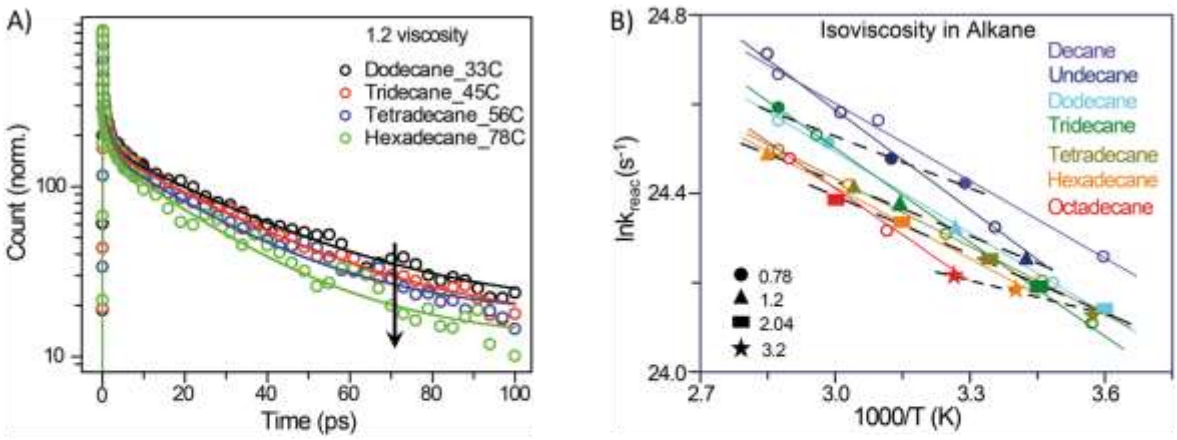

Figure 3. a) Fluorescence decay data recorded at 1.7 mPa s in a range of alkane solvents. The arrow indicates increasing temperature. b) Arrhenius and isoviscosity analyses in a series of alkane solvents; colors indicate different solvents. Arrhenius analyses are shown in open symbols and full lines for each individual solvent. Isoviscosities are shown by filled symbols and dashed lines, with each isoviscosity represented by a different symbol.

In figure 3 the isoviscosity data for the series of alkane solvents are shown, along with a temperature dependent decay measurement at a specific isoviscosity. In this case seven solvents were studied at a range of temperatures between 5 and 78 °C and all data were fit to a sum of two exponentials plus a fixed long (>1 ns) decay constant, accounting for the unresolved minor (ca 1%) slow components. The data are presented in the form of Arrhenius analyses, which are seen to be linear in any given single solvent (Figure 3B). The measurements at four different isoviscosities also have a linear relationship, but are of different slope to the single solvent data (Supporting Information Tables S3-4). The analyses shown in Figure 3 were applied to the longer (τ_2) of the two lifetime components recovered from the biexponential fit, but application of the same procedure to either the average relaxation time or to the short component (τ_1) alone gives essentially the same result (see SI Figure S1-S4).

That the slopes for the single solvent data compared with the isoviscosity data are different (Figure 3B), confirms the previously discussed role of viscosity in determining the reaction rate.[29] More significantly, isoviscosity data in these nonpolar solvents reveal the existence of an intrinsic activation barrier in the excited electronic state, along the $\mathbf{I_c}$ to $\mathbf{I_{mt}}$ reaction coordinate. The slopes yield a very low barrier of E_b =

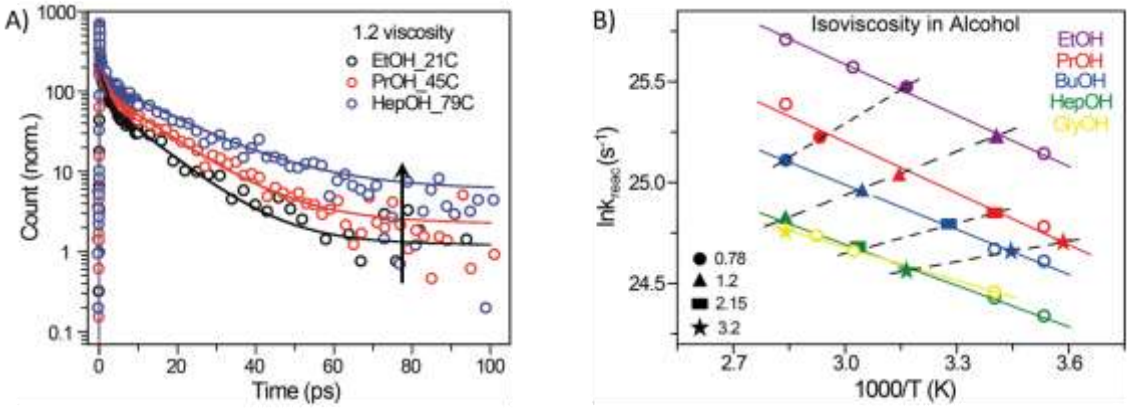

Figure 4. (a) Transient fluorescence data recorded at 1.2 mPa s in a range of alcohol solvents, where the arrow indicates increasing temperature b) Arrhenius and isoviscosity analyses in a series of alcohols solvents, with the meaning of the symbols as for Figure 3b.

3.4±0.5 kJ mol^{-1} (285 cm^{-1}); this is evidently sufficient to trap the excited state population in the missive region of the excited state surface for several picoseconds.

In Figure 4 the isoviscosity analysis for the series of n-alcohol solvents is presented along with a typical data set at one viscosity in a series of solvents. The Arrhenius analysis for each individual solvent again yields linear plots, with quite similar slopes (6.5 ± 0.7 kJ mol^{-1}) across the solvent series (see SI Table S6), which is consistent with there being no major specific solvent effect among the n-alcohols. Remarkably, analysis of the isoviscosity data recovers an accurately resolved but unphysical negative activation energy for all isoviscosities, in the range E_b = −2.8 to − 9.2 kJ mol^{-1}. This unexpected behavior is observed for both the longer lifetime component (presented in Figure 4) and the mean lifetime analyses (Supporting Information Figure S3-S4), and is clearly present in the data – for example at η = 1.2 mPa s there is a well resolved increasing lifetime with increasing temperature (Figure 4A).

The very different outcome of the isoviscosity analyses when applied at similar viscosities in n-alkane and n-alcohol solvents points to an additional factor determining the photoconversion of $\mathbf{I_c}$ to $\mathbf{I_{mt}}$. The data already suggest a distinct polarity effect, with the fluorescence decay time becoming markedly longer in non-polar solvent (Figure 2B) and also being longer in the less polar longer chain n-alcohols (Figure 4A). This polarity effect is confirmed in Figure 5 where we see that the Arrhenius analysis

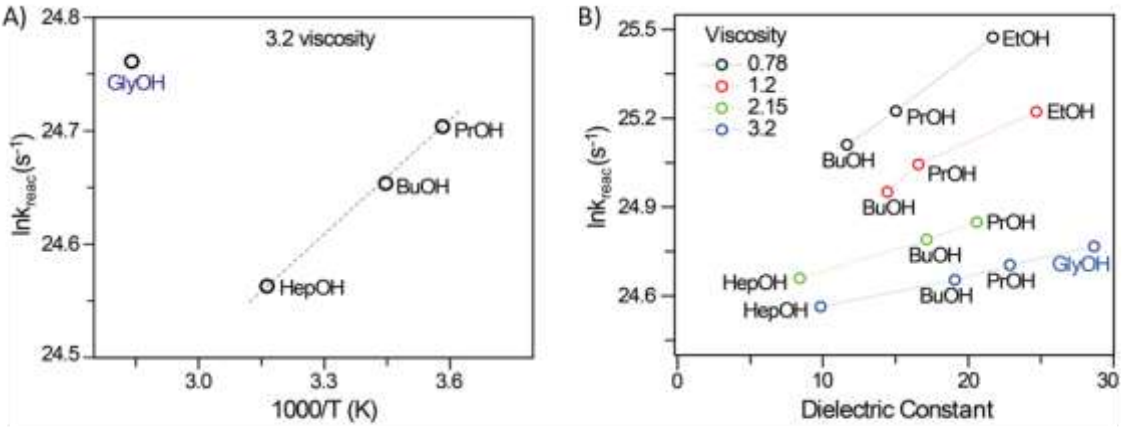

Figure 5. A) Comparison of the Arrhenius analysis in n-alcohols and a diol, showing anomalous effect of the diol. B) The same kinetic data as A) but plotted as a function of solvent dielectric constant.

conducted at the isoviscosity of 3.2 mPa s becomes nonlinear when the diol ethylene glycol is included (Figure 5A). In contrast, when these same lifetime data are plotted as a function of the solvent dielectric constant (the temperature dependence of which is tabulated in the region of interest[40-42]) the ethylene glycol data fit the same monotonic trend as the other solvents (Figure 5B). Hence, the reason for the exceptional behavior of the diol compared to the series of n-alcohols (Figure 5A) is that the diol is both polar and viscous, while for the n-alcohols, as viscosity increases towards that of the diol the polarity decreases. Whilst there is no reason *a priori* to expect a linear relationship between the solvent dielectric constant and lnk_{reac}, the consistent trend of decreasing lifetime in more polar media for any given isoviscosity (Figure 5B) is evidence of a role for solvent polarity in determining k_{reac}.

Polarity Dependence of the Isomerization Quantum Yield The isoviscosity analysis reveals a role for solvent polarity in controlling the excited state barrier crossing. A key question is whether this polarity dependent excited state process has a role in determining the final quantum yield of product formation. The yield was determined from analysis of the absorption spectra recorded after irradiation of $\mathbf{I_c}$ with a fixed dose of 355 nm radiation, with the number of photons absorbed being determined by actinometry; the methods are described in detail in supporting information. Sufficient time was allowed after irradiation to ensure quantitative conversion of the metastable form $\mathbf{I_{mt}}$ to the stable product, $\mathbf{I_t}$.

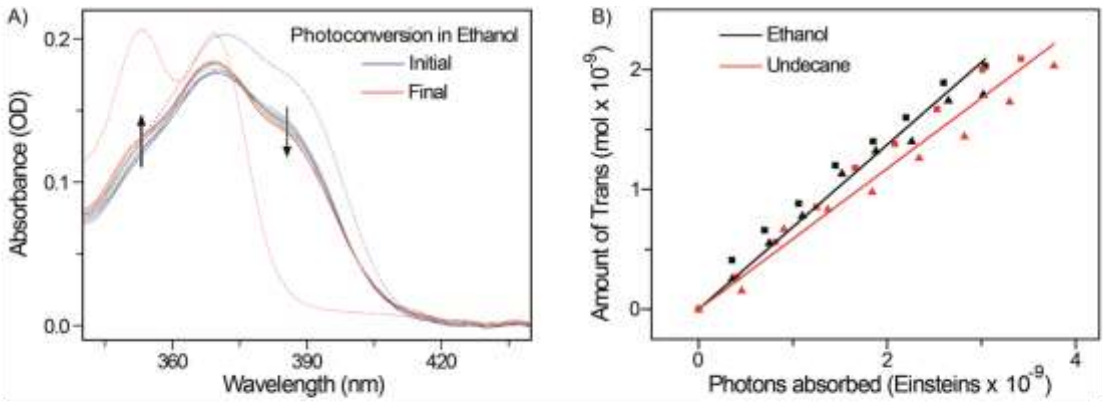

Figure 6. A) Irradiation dependent absorption spectra for I_c to I_t conversion in ethanol are given in solid line. The black arrow represent initial to final transition. Pure spectra for I_c and I_t are shown by dotted lines. B) Fits of the photoconversion yield in ethanol (black) and undecane (red) solvents.

The irradiation dependent spectra were analyzed in terms of the two known spectra of $\mathbf{I_c}$ and $\mathbf{I_t}$ (shown in Figure 6A). Again the polar ethanol and nonpolar undecane solvent were selected, because they have the same viscosities but very different polarities. The analysis of the data are shown in Figure 6B, yielding photochemical quantum yields of 0.69±0.06 for $\mathbf{I_c}$ in ethanol and 0.59±0.06 for undecane (see supporting information). While the absolute numbers differ from yields determined by other methods,[28] which may reflect the difficulty in determining quantum yield for systems where there is only a small change in absorption. It is apparent that the yield is not greatly altered by changing solvent polarity, and in particular the faster excited state decay in polar solvents does not correspond to a higher photoconversion rate.

Discussion

The isoviscosity analysis has (i) revealed an important role for solvent friction (viscosity) in controlling the excited state decay of $\mathbf{I_c}$ (ii) resolved the barrier height along the reactions coordinate as 3.4 ±0.5 kJ mol^{-1} in nonpolar solvents, providing an important parameter against which quantum chemical calculations of the excited state potential energy surface can be tested and (iii) revealed for the first time an important role for solvent polarity in modifying excited state dynamics. However, quantum

yield data show that the motor efficiency is not directly controlled by solvent polarity, suggesting it is not on its own a useful control parameter.

The polar solvent effect on the rate and fluorescence yield of $\mathbf{I_c}$ can be understood from a consideration of the excited state isomerization dynamics in molecules with ethylenic double bonds. Even the simplest example, ethylene, is predicted to exhibit charge separation along the isomerization coordinate, through the joint action of excited state electronic structure evolution and polar solvent dynamics.[43] For ethylene itself there are detailed calculations of the excited state dynamics.[44] The initially excited $\pi\pi^*$ state undergoes C=C bond torsion followed by pyramidalization at one of the C atoms. The out-of-plane distortion that results gives rise to a "sudden polarization", leading to a partial negative charge on the pyramidalizing C atom.[43] Closely related phenomena have been reported in a range of substituted ethylenes, and in well-established model compounds for excited state isomerization reactions,[35, 45-46] but its role has not, as far as we are aware, previously been noted for photomolecular motors.

In polar solvents this sudden increase in permanent dipole moment results in an excited state structure that can be stabilized through reorientation of polar residues in the solvation shell. The resulting decrease in energy of the charge transfer state can then lead to a change in the barrier to the isomerization.[35] Such solvent effects have been the topic of numerous investigations in simpler less sterically strained ethylenic systems, exemplified by stilbene trans to cis isomerization.[45, 47-48] In the present case the effect of the polar solvent is to accelerate the reaction, which corresponds to a suppression of the activation barrier. However, this is achieved without any substantial change in the energy of the emission spectrum *i.e*. no solvatochromic shifts in fluorescence are observed (Figure S6, Supporting Information). The absence of solvatochromism suggests that the charge separation does not occur in the emissive state of $\mathbf{I_c}$. Rather, it is the state formed after the barrier crossing that is stabilized by the polar solvent; it is this stabilization relative to the fluorescent state which leads to a reduction in

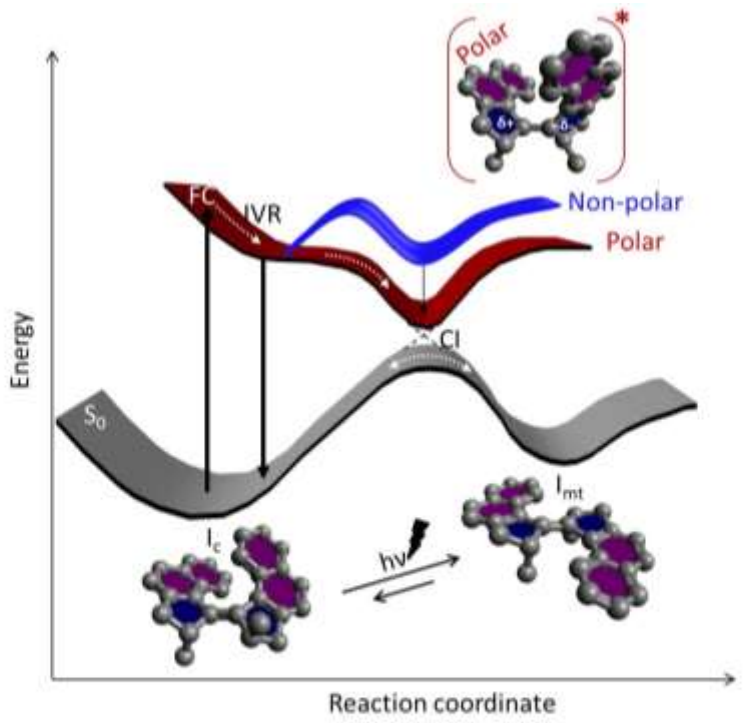

Figure 7 . Schematic potential surfaces for a photophysical model of the cis-to-trans isomerisation of first generation molecular motors. An initial 100 fs relaxation of the Franck Condon excited state populates the emissive state. In nonpolar solvent thermal reaction over a low barrier leads to conical intersection with the ground state. In polar solvent the charge separated excited state formed after the barrier is stabilized by subpicosecond solvent relaxation, suppressing the barrier and accelerating the reaction.

E_b without shifting the emission spectrum, as illustrated in Figure 7. The negative activation energy recovered from the isoviscosity analysis in the polar solvent (Figure 4) can then be understood as arising from two interrelated factors. First, the stabilization of the charge-separated configuration depends on the polarity of the solvent, which decreases from ethanol to heptanol, thus giving rise to different barriers along the series on n-alcohols. Second, the stabilization of the charge separated state to minimize the energy barrier requires solvent reorientation, which scales with the solvent's solvation correlation time, τ_S, which also increases between ethanol and heptanol (the mean τ_S increases from 15 to 250 ps, although in all solvents there is an ultrafast component[49]). Both of these effects will result in greater suppression of the barrier height in the more polar rapidly relaxing solvents, such that the effective barrier height is solvent dependent within the polar solvent series. Thus, the less viscous more polar short chain n-alcohols exhibit a faster decay at the lower temperatures, while for longer chain less

polar n-alcohols an elevated temperature is required to obtain the isoviscosity, but the polarity remains lower; these effects result in the longer fluorescence decay at higher temperatures, as observed (Figure 4).

Figure 7 presents a rationalization of the main observations of excited state dynamics, in terms of a one-dimensional excited state potential energy surface. Initial excitation of the $\pi\pi^*$ Franck-Condon state relaxes in 100 fs via a viscosity independent structural reorganization accompanied by IVR. This relaxation leads to the red shifted nonpolar emissive state. In nonpolar solvents, the conical intersection (CI) which ultimately leads to the vibrationally hot ground state, and subsequent branching between the product $\mathbf{I_{mt}}$ and the original ground state, is reached over a low barrier in the excited state. Progress over the barrier is resisted by solvent friction. This in turn suggest a reaction coordinate which displaces solvent, consistent with movement over the barrier involving torsion in the ethylenic bridging bond. Previous theoretical calculations on excited state dynamics in related molecular rotary motors have pointed to important roles for both C=C bond torsion and pyramidalization at a bridging carbon.[50-52] These are the modes which, at least in simpler systems, are known to lead to sudden polarization.[43] The sudden polarization will be coupled to ultrafast components of polar solvent reorientation, leading to stabilization of a twisted excited state with charge transfer character. This stabilization has the effect of reducing the barrier to the conical intersection with the ground state, thus accelerating the excited state decay of $\mathbf{I_c}$ in polar solvents. The one-dimensional representation of Figure 7 thus illustrates the main features of the excited state dynamics along a generalized reaction coordinate; we emphasize that the FC to fluorescent state relaxation and subsequent barrier crossing to the twisted CT state step will involve different intramolecular coordinates, and, at least the latter step, solvent reorganization; a quantitative understanding will require a multidimensional representation of the reaction coordinate.

One feature of the present results not readily accounted for in the one-dimensional representation of Figure 7 is the intrinsic multi-exponential fluorescence decay kinetics. The analysis of the time resolved

fluorescence required at least two components, with evidence of a weak unresolved slower component. There is no evidence, from NMR or Raman measurements for example, for a heterogeneous ground state population in $\mathbf{I_c}$, so the inhomogeneity must arise in the excited electronic state. Polar solvation dynamics can in principle contribute to a non-single exponential fluorescence decay, but the effects in $\mathbf{I_c}$ are observed equally in polar and nonpolar solvents, and the red-shift in emission and associated risetime on the red edge of the fluorescence, characteristic of solvation dynamics, are not seen.[53] Intramolecular vibrational redistribution may also contribute to a non-single exponential decay on the blue edge of the emission, but for $\mathbf{I_c}$ the biexponential decay persists right across the spectrum.[29] Quantum chemical calculations on related (second generation) molecular motors have reported multiple minima in the excited state potential energy surface, when plotted as a function of the torsion and pyramidalization coordinates.[50, 52] Further, these minima are separated by low barriers, which are in-turn separated by energy barriers of a few kcal mol^{-1} from distinct conical intersections between the excited and ground state singlets. Thus, one possible explanation for the multi-exponential decay is that different pathways to the conical intersection exist on this complex excited state surface, with different initial conformations being populated during subpicosecond IVR, following the ca 100 fs relaxation of the FC state to form the vibrationally hot fluorescence state. Further, these different excited state conformations may correspond to distinct radiative decay rates, and have different energies for the emission. A similar explanation was introduced to explain the dependence of the lifetime of the 'dark' state in a second generation motor on whether that state was populated from the stable or the metastable ground state.[25] Thus, we assign the multi-exponential (and wavelength dependent) decay of the emission to an inhomogeneous structural distribution in the emissive state of $\mathbf{I_c}$, where each population has distinct radiationless and radiative decay rates.

The viscosity dependence in nonpolar solvents can be analyzed to extract further information on the reaction coordinate. In order to isolate the frictional effect of nonpolar solvent on photo-isomerization,

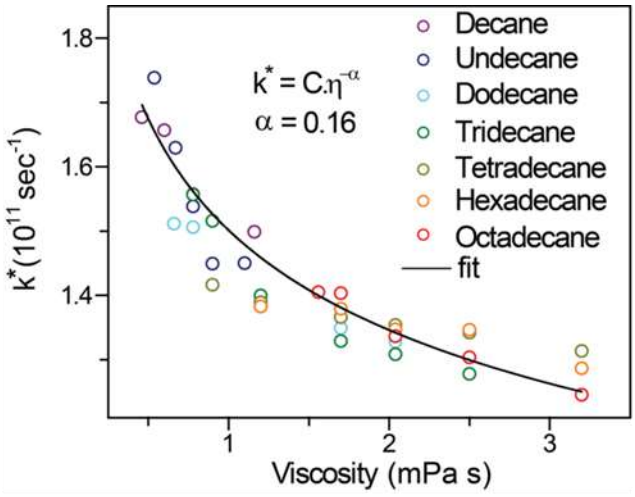

Figure 8. Kramer's analysis of $\mathbf{I_c}$ decay in nonpolar solvents in intermediate viscosity regime.

the contributions from the (thermal) barrier crossing process can be removed, resulting in the reduced rate constant, *k**:[32]

$$k^* = k_{reac} exp\left(\frac{E_b}{RT}\right) = F(\eta) \qquad (3)$$

The value of E_b is obtained from the isoviscosity plot in Figure 3. Since the viscosity dependence of the internal barrier is not significant (see supplementary information Table S3), the average value of E_b = 3.41 kJ mol^{-1} is used for determination of *k**. The *k** values calculated for the series of nonpolar solvents all fall on a common line, and scale with the viscosity (Figure 8). However, an attempt to fit these data to Kramers equation (2) was not successful, as the curvature in the data was greater than predicted by (2). An alternative approach is to fit the reduced rate constant to a fractional viscosity dependence, k^*=C $\eta^{-\alpha}$ where the value of α provides information on the barrier crossing process. Figure 8 shows the result of the fit yielding α = 0.16. Such fractional power dependencies are predicted in the frequency dependent friction theory of Grote and Hynes.[38] In GH theory a value α = 1 corresponds to a barrier crossing in the Smoluchowski limit, while for 0.1<α<1 the barrier crossing reflects frequency dependent friction. The data for $\mathbf{I_c}$ clearly deviate from the Smoluchowski limit. Further modelling in terms of Grote - Hynes theory requires experimental measurements over a wider viscosity range, a more detailed picture of both solvent – solute collisions (accessible from molecular dynamics simulation) and details on the

shape of the potential energy surface near the barrier (requiring quantum mechanical calculations on **I**). These are not presently available, restricting us to the qualitative conclusion that, even in the nonpolar solvents, the details of the solvent – solute interaction and the shape of the potential barrier are critical in determining excited state dynamics of $\mathbf{I_c}$.

A final important question is the extent to which the observed effect of solvent polarity on the shape of the excited state potential energy surface influences the photochemical cross section. There are a number of earlier studies comparing solvent effects on excited state decay time and cis-trans isomerization quantum yield. For 1,2-di(1-methyl-2-naphthyl)ethane a decreasing quantum yield correlated with an increasing trans to cis isomerization,[54] while for a series of aminostilbenes a shorter excited stat lifetime in polar solvents correlated with a lower isomerization yield[55]. For cis-stilbene itself the lifetime is shorter in polar solvents but the isomerization yield is a weak function of polarity (but the case is complicated by the photochemical ring closure reaction, while for trans stilebene the yield is reported to be independent of solvent, while the lifetime varies with polarity and viscosity.[56-57] In the present case, increasing solvent polarity quenches the excited state lifetime by suppressing the barrier to radiationless decay, the final yield of the isomerization reaction was observed to be only weakly dependent on solvent polarity, similar to the case for trans stilbene. This suggests that the primary factor influencing the isomerization yield is not the decay of the emissive state, or even the shape of the excited state surface. That the isomerization yield is not a function of the excited state decay suggests that the steps determining the yield must occur later in the relaxation, possibly in the vibrationally hot ground state formed after internal conversion. There is ample evidence in other excited state isomerization reactions that the internal conversion can itself be modified by the solvent, effecting the photochemical yield.[58-60] Apparently in $\mathbf{I_c}$ these effects are washed out after internal conversion. This might occur if there is a relatively long lived hot ground state, such that the memory of the state formed immediately after internal conversion is lost. In future work we will investigate the effect of electron

withdrawing and donating groups conjugated to the bridging double bond, which may promote the role of CT states and the role of solvent polarity.

Conclusions

The excited state decay kinetics of the first generation unidirectional molecular motor $\mathbf{I_c}$ have been analyzed through ultrafast time resolved fluorescence. An isoviscosity analysis in nonpolar solvents reveals a low barrier to the radiationless decay pathway. The barrier crossing is resisted by increasing solvent viscosity, but the process is far from the Smoluchowski limit. Instead, a fractional power dependence on viscosity was observed, consistent with a role for frequency dependent friction, *i.e.* the shape of the barrier and the details of the solvent - solute collision are important in determining the reaction rate. The same isoviscosity analysis in polar solvents formally yields an unphysical negative activation energy. This result is traced to a solvent dependence of the barrier height, with the barrier being suppressed in polar media. The physical origin of this is likely to be the sudden polarization which develops along the reaction coordinate in the excited state isomerization of ethylenic double bonds. The weak solvent effect on electronic spectra suggests that the polarization develops after the barrier. The solvent dependence of the excited state dynamics suggested the need for an examination of the role of polarity in determining the quantum yield for isomerization. The yield was shown not to be a strong function of solvent polarity. This result was discussed in terms of a potential role for a vibrationally hot ground state intermediate in determining the final step in the photochemical reaction.

Supporting Information. The Supporting Information is available free of charge.
Additional experimental details, photochemical quantum yields measurements, detailed numerical tables from fitting of the time-resolved data, and additional Figures (PDF).

Notes

The authors declare no competing financial interest.

Acknowledgements

This work was supported financially by the EPSRC (grants to SRM, EP/R042357/1, EP/J009148/1), the Netherlands Organization for Scientific Research (NWO-CW to WRB, BLF), the European Research Council (ERC, advanced grant no. 694345 to BLF), the Ministry of Education, Culture and Science (Gravitation Program no. 024.001.035 to WRB, BLF).

References:

1. Kinbara, K.; Aida, T., Toward Intelligent Molecular Machines: Directed Motions of Biological and Artificial Molecules and Assemblies. *Chemical Reviews* **2005**, *105*, 1377-1400.
2. Coskun, A.; Banaszak, M.; Astumian, R. D.; Stoddart, J. F.; Grzybowski, B. A., Great Expectations: Can Artificial Molecular Machines Deliver on Their Promise? *Chemical Society Reviews* **2012**, *41*, 19-30.
3. Roke, D.; Wezenberg, S. J.; Feringa, B. L., Molecular Rotary Motors: Unidirectional Motion around Double Bonds. *Proceedings of the National Academy of Sciences* **2018**, *115*, 9423-9431.
4. Kassem, S.; van Leeuwen, T.; Lubbe, A. S.; Wilson, M. R.; Feringa, B. L.; Leigh, D. A., Artificial Molecular Motors. *Chemical Society Reviews* **2017**, *46*, 2592-2621.
5. Balzani, V.; Credi, A.; Venturi, M., Light Powered Molecular Machines. *Chemical Society Reviews* **2009**, *38*, 1542-1550.
6. Baroncini, M.; Silvi, S.; Credi, A., Photo- and Redox-Driven Artificial Molecular Motors. *Chemical Reviews* **2020**, *120*, 200-268.
7. Kay, E. R.; Leigh, D. A.; Zerbetto, F., Synthetic Molecular Motors and Mechanical Machines. *Angewandte Chemie-International Edition* **2007**, *46*, 72-191.
8. García-López, V.; Liu, D.; Tour, J. M., Light-Activated Organic Molecular Motors and Their Applications. *Chemical Reviews* **2020**, *120*, 79-124.
9. van Leeuwen, T.; Lubbe, A. S.; Stacko, P.; Wezenberg, S. J.; Feringa, B. L., Dynamic Control of Function by Light-Driven Molecular Motors. *Nature Reviews Chemistry* **2017**, *1*.
10. Norikane, Y.; Tamaoki, N., Light-Driven Molecular Hinge: A New Molecular Machine Showing a Light-Intensity-Dependent Photoresponse That Utilizes the Trans-Cis Isomerization of Azobenzene. *Org. Lett.* **2004**, *6*, 2595-2598.
11. Muraoka, T.; Kinbara, K.; Aida, T., Mechanical Twisting of a Guest by a Photoresponsive Host. *Nature* **2006**, *440*, 512-515.
12. Feringa, B. L., In Control of Motion: From Molecular Switches to Molecular Motors. *Accounts of Chemical Research* **2001**, *34*, 504-513.
13. Koumura, N.; Zijlstra, R. W. J.; van Delden, R. A.; Harada, N.; Feringa, B. L., Light-Driven Monodirectional Molecular Rotor. *Nature* **1999**, *401*, 152-155.
14. ter Wiel, M. K. J.; van Delden, R. A.; Meetsma, A.; Feringa, B. L., Increased Speed of Rotation for the Smallest Light-Driven Molecular Motor. *Journal of the American Chemical Society* **2003**, *125*, 15076-15086.

15. Koumura, N.; Geertsema, E. M.; van Gelder, M. B.; Meetsma, A.; Feringa, B. L., Second Generation Light-Driven Molecular Motors. Unidirectional Rotation Controlled by a Single Stereogenic Center with near-Perfect Photoequilibria and Acceleration of the Speed of Rotation by Structural Modification. *Journal of the American Chemical Society* **2002**, *124*, 5037-5051.
16. Pathem, B. K.; Claridge, S. A.; Zheng, Y. B.; Weiss, P. S., Molecular Switches and Motors on Surfaces. *Annual Review of Physical Chemistry, Vol 64* **2013**, *64*, 605-630.
17. Browne, W. R.; Feringa, B. L., Light Switching of Molecules on Surfaces. *Annual Review of Physical Chemistry* **2009**, *60*, 407-428.
18. Pollard, M. M.; Meetsma, A.; Feringa, B. L., A Redesign of Light-Driven Rotary Molecular Motors. *Organic & Biomolecular Chemistry* **2008**, *6*, 507-512.
19. Klok, M.; Boyle, N.; Pryce, M. T.; Meetsma, A.; Browne, W. R.; Feringa, B. L., Mhz Unidirectional Rotation of Molecular Rotary Motors. *Journal of the American Chemical Society* **2008**, *130*, 10484-+.
20. Conyard, J.; Cnossen, A.; Browne, W. R.; Feringa, B. L.; Meech, S. R., Chemically Optimizing Operational Efficiency of Molecular Rotary Motors. *Journal of the American Chemical Society* **2014**, *136*, 9692-9700.
21. Klok, M.; Janssen, L.; Browne, W. R.; Feringa, B. L., The Influence of Viscosity on the Functioning of Molecular Motors. *Faraday Discussions* **2009**, *143*, 319-334.
22. Pollard, M. M.; Klok, M.; Pijper, D.; Feringa, B. L., Rate Acceleration of Light-Driven Rotary Molecular Motors. *Advanced Functional Materials* **2007**, *17*, 718-729.
23. Ikeda, T.; Dijkstra, A. G.; Tanimura, Y., Modeling and Analyzing a Photo-Driven Molecular Motor System: Ratchet Dynamics and Non-Linear Optical Spectra. *Journal of Chemical Physics* **2019**, *150*.
24. Klok, M.; Browne, W. R.; Feringa, B. L., Kinetic Analysis of the Rotation Rate of Light-Driven Unidirectional Molecular Motors. *Physical Chemistry Chemical Physics* **2009**, *11*, 9124-9131.
25. Hall, C. R.; Browne, W. R.; Feringa, B. L.; Meech, S. R., Mapping the Excited-State Potential Energy Surface of a Photomolecular Motor. *Angewandte Chemie-International Edition* **2018**, *57*, 6203-6207.
26. Hall, C. R.; Conyard, J.; Heisler, I. A.; Jones, G.; Frost, J.; Browne, W. R.; Feringa, B. L.; Meech, S. R., Ultrafast Dynamics in Light-Driven Molecular Rotary Motors Probed by Femtosecond Stimulated Raman Spectroscopy. *Journal of the American Chemical Society* **2017**, *139*, 7408-7414.
27. Conyard, J.; Addison, K.; Heisler, I. A.; Cnossen, A.; Browne, W. R.; Feringa, B. L.; Meech, S. R., Ultrafast Dynamics in the Power Stroke of a Molecular Rotary Motor. *Nature Chemistry* **2012**, *4*, 547-551.
28. Wiley, T. E.; Konar, A.; Miller, N. A.; Spears, K. G.; Sension, R. J., Primed for Efficient Motion: Ultrafast Excited State Dynamics and Optical Manipulation of a Four Stage Rotary Molecular Motor. *The Journal of Physical Chemistry A* **2018**, *122*, 7548-7558.
29. Sardjan, A. S.; Roy, P.; Danowski, W.; Bressan, G.; Nunes dos Santos Comprido, L.; Browne, W. R.; Feringa, B. L.; Meech, S. R., Ultrafast Excited State Dynamics in a First Generation Photomolecular Motor. *Chemphyschem* **2020**, *21*, 594-599.
30. Vauthey, E., Isomerization Dynamics of a Thiacarbocyanine Dye in Different Electronic States and in Different Classes of Solvents. *Chemical Physics* **1995**, *196*, 569-582.
31. Todd, D. C.; Fleming, G. R., Cis-Stilbene Isomerization - Temperature-Dependence and the Role of Mechanical Friction. *Journal of Chemical Physics* **1993**, *98*, 269-279.
32. Velsko, S. P.; Waldeck, D. H.; Fleming, G. R., Breakdown of Kramers Theory Description of Photochemical Isomerization and the Possible Involvement of Frequency Dependent Friction. *The Journal of Chemical Physics* **1983**, *78*, 249-258.
33. Zijlstra, R. W. J.; van Duijnen, P. T.; Feringa, B. L.; Steffen, T.; Duppen, K.; Wiersma, D. A., Excited-State Dynamics of Tetraphenylethylene: Ultrafast Stokes Shift, Isomerization, and Charge Separation. *Journal of Physical Chemistry A* **1997**, *101*, 9828-9836.

34. Lenderink, E.; Duppen, K.; Wiersma, D. A., Femtosecond Twisting and Coherent Vibrational Motion in the Excited-State of Tetraphenylethylene. *Journal of Physical Chemistry* **1995**, *99*, 8972-8977.
35. Mohrschladt, R.; Schroeder, J.; Schwarzer, D.; Troe, J.; Vohringer, P., Barrier Crossing and Solvation Dynamics in Polar-Solvents - Photoisomerization of Trans-Stilbene and E,E-Diphenylbutadiene in Compressed Alkanols. *Journal of Chemical Physics* **1994**, *101*, 7566-7579.
36. Heisler, I. A.; Kondo, M.; Meech, S. R., Reactive Dynamics in Confined Liquids: Ultrafast Torsional Dynamics of Auramine O in Nanoconfined Water in Aerosol Ot Reverse Micelles. *Journal of Physical Chemistry B* **2009**, *113*, 1623-1631.
37. Crosson, S.; Rajagopal, S.; Moffat, K., The Lov Domain Family: Photoresponsive Signaling Modules Coupled to Diverse Output Domains†. *Biochemistry* **2002**, *42*, 2-10.
38. Hynes, J. T., Chemical-Reaction Rates and Solvent Friction. *Journal of Statistical Physics* **1986**, *42*, 149-168.
39. Park, N. S.; Waldeck, D. H., Implications for Multidimensional Effects on Isomerization Dynamics: Photoisomerization Study of 4,4'-Dimethylstilbene in N-Alkane Solvents. *The Journal of Chemical Physics* **1989**, *91*, 943-952.
40. Bezman, R. D.; Casassa, E. F.; Kay, R. L., The Temperature Dependence of the Dielectric Constants of Alkanols. *Journal of Molecular Liquids* **1997**, *73-74*, 397-402.
41. Zahn, M.; Ohki, Y.; Fenneman, D. B.; Gripshover, R. J.; Gehman, V. H., Dielectric Properties of Water and Water/Ethylene Glycol Mixtures for Use in Pulsed Power System Design. *Proceedings of the IEEE* **1986**, *74*, 1182-1221.
42. Vij, J. K.; Scaife, W. G.; Calderwood, J. H., The Pressure and Temperature Dependence of the Complex Permittivity of Heptanol Isomers. *Journal of Physics D: Applied Physics* **1981**, *14*, 733-746.
43. Brooks, B. R.; Schaefer, H. F., Sudden Polarization: Pyramidalization of Twisted Ethylene. *Journal of the American Chemical Society* **1979**, *101*, 307-311.
44. Ben-Nun, M.; Martínez, T. J., Photodynamics of Ethylene: Ab Initio Studies of Conical Intersections. *Chemical Physics* **2000**, *259*, 237-248.
45. Waldeck, D. H., Photoisomerization Dynamics of Stilbenes. *Chemical Reviews* **1991**, *91*, 415-436.
46. Schuurman, M. S.; Stolow, A., Dynamics at Conical Intersections. *Annual Review of Physical Chemistry* **2018**, *69*, 427-450.
47. Kumpulainen, T.; Lang, B.; Rosspeintner, A.; Vauthey, E., Ultrafast Elementary Photochemical Processes of Organic Molecules in Liquid Solution. *Chemical Reviews* **2017**, *117*, 10826-10939.
48. Sivakumar, N.; Hoburg, E. A.; Waldeck, D. H., Solvent Dielectric Effects on Isomerization Dynamics: Investigation of the Photoisomerization of 4,4'-Dimethoxystilbene and T-Stilbene in N-Alkyl Nitriles. *The Journal of Chemical Physics* **1989**, *90*, 2305-2316.
49. Horng, M. L.; Gardecki, J. A.; Papazyan, A.; Maroncelli, M., Subpicosecond Measurements of Polar Solvation Dynamics: Coumarin 153 Revisited. *The Journal of Physical Chemistry* **1995**, *99*, 17311-17337.
50. Kazaryan, A.; Lan, Z.; Schafer, L. V.; Thiel, W.; Filatov, M., Surface Hopping Excited-State Dynamics Study of the Photoisomerization of a Light-Driven Fluorene Molecular Rotary Motor. *Journal of Chemical Theory and Computation* **2011**, *7*, 2189-2199.
51. Kazaryan, A.; Kistemaker, J. C. M.; Schafer, L. V.; Browne, W. R.; Feringa, B. L.; Filatov, M., Understanding the Dynamics Behind the Photoisomerization of a Light-Driven Fluorene Molecular Rotary Motor. *Journal of Physical Chemistry A* **2010**, *114*, 5058-5067.
52. Kazaryan, A.; Filatov, M., Density Functional Study of the Ground and Excited State Potential Energy Surfaces of a Light-Driven Rotary Molecular Motor (3r,3'R)-(P,P)-Trans-1,1',2,2',3,3',4,4'-Octahydro-3,3'-Dimethyl-4,4'-Biphenanthrylidene. *The Journal of Physical Chemistry A* **2009**, *113*, 11630-11634.

53. Horng, M. L.; Gardecki, J. A.; Papazyan, A.; Maroncelli, M., Subpicosecond Measurements of Polar Solvation Dynamics - Coumarin-153 Revisited. *Journal of Physical Chemistry* **1995**, *99*, 17311-17337.
54. Saltiel, J.; Kumar, V. K. R.; Redwood, C. E.; Mallory, F. B.; Mallory, C. W., Competing Adiabatic and Nonadiabatic Pathways in the Cis–Trans Photoisomerization of Cis-1,2-Di(1-Methyl-2-Naphthyl)Ethene. A Zwitterionic Twisted Intermediate. *Photochemical & Photobiological Sciences* **2014**, *13*, 172-181.
55. Lewis, F. D.; Kalgutkar, R. S.; Yang, J.-S., The Photochemistry of Trans-Ortho-, -Meta-, and -Para-Aminostilbenes. *Journal of the American Chemical Society* **1999**, *121*, 12045-12053.
56. Rodier, J. M.; Myers, A. B., Cis-Stilbene Photochemistry: Solvent Dependence of the Initial Dynamics and Quantum Yields. *Journal of the American Chemical Society* **1993**, *115*, 10791-10795.
57. Sundström, V.; Gillbro, T., Dynamics of the Isomerization of Trans-Stilbene in N-Alcohols Studied by Ultraviolet Picosecond Absorption Recovery. *Chem. Phys. Lett.* **1984**, *109*, 538-543.
58. Malhado, J. P.; Spezia, R.; Hynes, J. T., Dynamical Friction Effects on the Photoisomerization of a Model Protonated Schiff Base in Solution. *The Journal of Physical Chemistry A* **2011**, *115*, 3720-3735.
59. Malhado, J. P.; Hynes, J. T., Photoisomerization for a Model Protonated Schiff Base in Solution: Sloped/Peaked Conical Intersection Perspective. *The Journal of Chemical Physics* **2012**, *137*, 22A543.
60. Ben-Nun, M.; Molnar, F.; Schulten, K.; Martínez, T. J., The Role of Intersection Topography in Bond Selectivity of <Em>Cis-Trans</Em> Photoisomerization. *Proceedings of the National Academy of Sciences* **2002**, *99*, 1769-1773.

TOC Graphic